Helium-atom diffraction study of the submonolayer structures of sodium on Cu(001)

Andrew P. Graham and J. Peter Toennies
M.P.I. für Strömungsforschung, Bunsenstraße 10, D-37073 Göttingen, Germany
(Received 19 June 1997)

The structure and low-frequency vibrations of submonolayer coverages of sodium adsorbed on Cu(001) have been investigated using high-resolution helium-atom diffraction and time-of-flight measurements at $T_s = 50$ and 100 K. At low coverages, $\Theta_{Na} \lesssim 0.2$, the overlayer structures are determined by a strong repulsive interaction between neighboring sodium atoms, while the low-energy vibrations are characterized by a parallel frustrated translation mode (T-mode) frequency of $\hbar\omega \sim 6$ meV. At higher coverages, $\Theta_{Na} \gtrsim 0.2$, a series of quasi-one-dimensional structures are observed, and are accompanied by a substantial lowering of the T-mode frequency to $\hbar\omega \sim 2$ meV. The diffraction patterns and low T-mode frequencies strongly indicate that the sodium atoms form one-dimensional islands in this coverage range. [S0163-1829(97)06747-7]

I. INTRODUCTION

The structure and properties of submonolayer coverages of alkali-metal atoms on metal surfaces have been extensively studied experimentally.[1–3] These results have stimulated a wide range of theoretical studies of the different interactions involved.[4–6] Despite the relatively simple electronic structure of alkali-metal atoms in the gas phase, the observed structures have been found to be surprisingly complicated. For different alkali-metal–substrate combinations, a fascinating array of structures have been observed, as discussed in two recent review articles by Diehl and McGrath.[1,2] At low temperatures, $T_s \lesssim 200$ K, low coverages of most alkali-metal atoms adsorbed on dense surfaces [e.g., fcc(001), fcc(111)] do not alloy,[7] and show a range of quasihexagonal overlayer structures in which the distance between the atoms is maximized.[8] The repulsive interactions are attributed to the large dipole moments formed on the alkali metal due to partial ionization on adsorption, as indicated by a strong decrease of the work function.[9] It is generally assumed that the competition between the many-body repulsive dipole-dipole interactions and the local adsorption potentials determines whether the structures are commensurate or not. As the monolayer approaches completion, most systems show a uniform compression of the quasihexagonal structure up to the complete monolayer density, while several systems have shown island formation or reconstruction of the substrate atoms. At the completion of the monolayer, the surface is typically metallic in nature, indicating that a transition from ionic to metallic bonding has taken place during growth of the first layer.[10] In this connection it should be noted that the coverage of a monolayer depends on the structure of the layer and may, for some systems, be less than unity. In the present case of Na/Cu(001) the monolayer coverage is $\Theta_{Na} = 0.5$.[11]

Sodium on Cu(001) has been the subject of several experimental studies. In addition to the now standard measurements of the change of the work function with coverage,[11] both the perpendicular vibration frequency of the sodium atoms with respect to the surface (S mode),[12] as well as the parallel frustrated translation vibrational mode frequency (T mode),[13] have been measured recently. Very recently, quasielastic helium-atom scattering has been used to study the microscopic diffusional motion of the sodium atoms, and yields a very low value of the diffusion barrier of $E_{diff} = 51 \pm 6$ meV and a diffusion coefficient of $D = 8 \times 10^{-5}$ cm^2 s^{-1} at room temperature. In addition, vibrations of thicker sodium layers have been investigated.[14,15] Some of these dynamical properties are summarized in Table I for later reference.

Most previous structural studies have been based on low-energy electron-diffraction (LEED) measurements. For coverages of less than $\Theta_{Na} \lesssim 0.2$, measured with respect to the Cu(001) surface-atom density, halos around the diffraction peaks have been reported at a temperature of $T_s = 180$ K.[11] At the same temperature and higher coverages, the diffraction pattern changed to a $c(14\times2)$ structure for $\Theta_{Na} \sim 0.3$, while for coverages between $\Theta_{Na} \sim 0.3$ and completion of the monolayer at $\Theta_{Na} = 0.5$, a $c(2\times2)$ diffraction pattern was observed.[11] A fourfold hollow adsorption site was deduced for the $c(2\times2)$ surface from an analysis of LEED I-V curves.[11] The observation of relatively few distinct intermediate structures for Na/Cu(001) at room temperature is probably due to the high mobility of sodium atoms, allowing them to diffuse rapidly on the surface.

At low temperatures the competition between the local substrate holding potential and the strong dipole-dipole repulsions, resulting from the large dipole moment of $\mu_0 = 2.8$ D,[16] is expected to lead to a more complex phase diagram. As pointed out by Diehl and McGrath in their recent reviews[1,2] up to now little is known about these low temperature structures. To address this deficit, helium-atom scattering (HAS) has been used in the present study to characterize the submonolayer ($\Theta_{Na} \lesssim 0.5$) structure and low-frequency vibrational dynamics of sodium on Cu(001) adsorbed at a surface temperature of $T_s = 200$ K and subsequently cooled to the lower temperatures of $T_s = 50$ and 100 K. HAS is particularly suitable for this type of study due to (a) its special surface sensitivity resulting from the relatively large scattering cross section of helium atoms for most adsorbates on metal surfaces,[17] and (b) the possibility to use time-of-flight techniques to measure the low-frequency adsorbate vibrations.[19]

The present helium diffraction patterns at low coverages

TABLE I. Some experimentally determined physical properties of sodium atoms adsorbed on Cu(001).

Property	Value	Units	Reference
S mode ($\hbar\omega_\perp$)	19[a]	meV	12
T mode ($\hbar\omega_\parallel$)	5.6[b]	meV	13
Diffusion barrier $E_{\rm diff}$	51 ± 6	meV	13
Diffusion prefactor D_0[c]	6×10^{-4}	cm^2/s	13
Dipole moment μ_0	2.8	D	16
Polarizability α	17.6	$Å^3$	16
Monolayer density $c(2\times2)\Theta_{\rm Na}=0.5$	7.65×10^{18}	m^{-2}	11

[a]Measured for a surface temperature $T_s=300$ K (Ref. 12).
[b]Measured for a surface temperature $T_s=180$ K and a coverage of $\Theta_{\rm Na}=0.1$ (Ref. 13).
[c]D_0 was derived from an exponential fit of the diffusion coefficient $D=D_0\exp(E_{\rm diff}/k_BT_s)$.

($\Theta_{\rm Na}\lesssim0.2$) confirm the importance of sodium-sodium repulsions in determining the observed superstructures, as anticipated from the structures on other alkali-metal–fcc(001) surfaces.[2] A $c(4\sqrt{2}\times2\sqrt{2})R45°$ was observed for a coverage of $\Theta_{\rm Na}=0.125$, while a $\begin{pmatrix}3&0\\-2&2\end{pmatrix}$ unit cell was seen for $\Theta_{\rm Na}=0.16$, both indicating a quasihexagonal arrangement of the sodium atoms compatible with a dominant repulsive interaction. The T mode, observed previously for isolated sodium atoms at $\Theta_{\rm Na}\sim0.1$ and measured to be $\hbar\omega=6$ meV for $T_s=50$ K and $\Theta_{\rm Na}=0.048$ in the present work, was found to persist up to $\Theta_{\rm Na}\approx0.2$. The lack of multiple or significantly broadened inelastic peaks suggests that the sodium atoms occupy equivalent adsorption sites on the surface up to this coverage. At higher coverages, $\Theta\gtrsim0.2$, a series of one-dimensional structures, not previously reported for any of the alkali metals on fcc(001) metals, were observed. The formation of these structures is found to be accompanied by an increase of the work function and a significantly lowered T-mode frequency, indicating either a change in the adsorption site or, more probably, a change in the nature of the sodium-copper bond, possibly corresponding to a one-dimensional metalization. For later reference, the Cu(001) surface is shown schematically in Fig. 1, where the important directions and distances are indicated.

This paper is organized in the following way: In Sec. II, details of the experimental apparatus are presented. Following that, in Sec. III, the HAS results are shown and the results are then discussed in conjunction with previous studies in Sec. IV. The main conclusions of this work are reported in Sec. V.

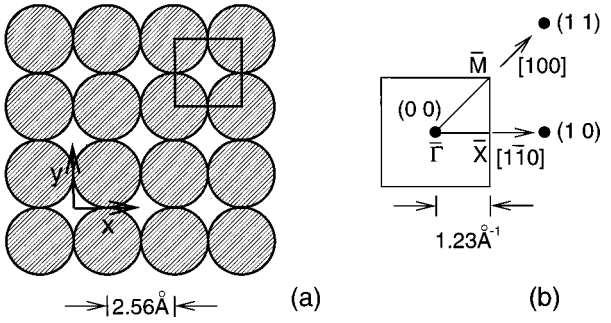

FIG. 1. Schematic diagram showing the structure of the Cu(001) surface. The real space (a) and the first Brillouin zone of the reciprocal space (b) lattices are indicated. The two scattering azimuths [100] and [110] used in the present study are shown. From LEED studies, it has been established that the Na atoms occupy the fourfold hollow sites (Ref. 11).

II. EXPERIMENT

The HUGO II high-resolution HAS system[20,21] incorporates a supersonic atomic helium beam source of $\Delta v/v\sim1\%$, a target chamber which has a base pressure of less than 2×10^{-11} mbar, and a time-of-flight arm of 1.4-m length at a total scattering angle of $\theta_{\rm SD}=95.8°$ with respect to the incident beam. Two orthogonal components of the parallel wave vector transfer to the surface, ΔK_x and ΔK_y, were scanned in these measurements by rotating the sample in the scattering plane by an angle $\Delta\theta$ away from the specular and tilting it by an angle ϕ out of the scattering plane:

$$\Delta K_x=-2k_i\sin(\Delta\theta)\cos(\theta_{\rm SD}/2), \tag{1}$$

$$\Delta K_y=k_i\sin(\phi)[\cos(\theta_{\rm SD}/2-\Delta\theta)+\cos(\theta_{\rm SD}/2+\Delta\theta)], \tag{2}$$

where k_i is the incident momentum of the helium atoms. Thus the complete two-dimensional (2D) parallel momentum-transfer space could be mapped out systematically by changing $\Delta\theta$ and ϕ with the sample manipulator. ΔK_x is dependent only on the polar angle $\Delta\theta$, and is independent of the tilt angle. The value of ΔK_y at a particular tilt angle is, however, weakly dependent on the polar angle $\Delta\theta$ used, due to the cosine terms in Eq. (2). This dependence leads to a slight distortion of the measured diffraction pattern when plotted as function of polar and tilt angles, essentially making the diffraction peaks further apart in tilt angle for larger values of $|\Delta\theta|$. Since the distortion is small, the 2D angular distributions are presented as measured.

The copper single crystal was first aligned along the (001) direction to within an accuracy of better than 0.25°, and then cut and mechanically polished. In vacuum, the surface was then cleaned with repeated cycles of sputtering and annealing until no contamination could be detected with Auger spectroscopy ($\Theta<0.005$), and elastic and inelastic helium scattering showed a smooth surface with a high degree of order. The sample temperature was controlled to well within ±1 K with an absolute accuracy of ±5 K using a Ni-CrNi (K type) thermocouple attached to the side of the copper sample.

Sodium was evaporated from a SAES Getters alkali-metal source directed normal to the sample surface at a distance of 5 cm. The metal source was carefully outgassed prior to use, so that the base pressure in the target chamber did not rise above 1×10^{-10} mbar during evaporation. During the dispenser warm-up cycle (typically 2 min), and during adsorption the surface was held at a temperature of $T_s=200$ K to prevent CO and H_2O, two of the main vacuum contaminants, from sticking to the Cu(001) surface. The sodium coverage was monitored during deposition via the decrease of the specular helium reflectivity.[17] The sodium coverage scale was calibrated with an absolute accuracy of ~0.005 using the $c(2\times2)$ diffraction structure [$\Theta_{Na}=0.5$ (Ref. 11)], and assuming a constant sticking coefficient.[18]

Prior to the HAS measurements the Na/Cu(001) surface was cooled by a liquid He cold finger to $T_s=50$ K (100 K) in order to reduce the diffusional motion of the sodium atoms. By extrapolating the results of Ellis and Toennies,[13] the diffusion rate is estimated to be reduced from $D\approx3\times10^{-5}$ cm^2/s at $T_s=200$ K, to $D\approx4\times10^{-9}$ cm^2/s at $T_s=50$ K for a coverage of $\Theta_{Na}=0.1$. Thus a lower temperature could be used in order to improve the long-range order of the sodium overlayer, so that sharper diffraction features could be observed and, consequently, make interpretation of the interactions easier. It is anticipated that there is very little difference between measurements performed on a surface prepared at a temperature of $T_s=50$ K, and one prepared at $T_s=200$ K and subsequently cooled to $T_s=50$ K.

III. RESULTS

A. Specular reflectivity measurements

Figure 2 compares the variation of the work function $\Delta\Phi$ as determined by Mizuno in Ref. 11 [Fig. 2(a)], with the normalized specular helium signal I/I_0 as a function of sodium coverage at a surface temperature of $T_s=40$ K [Fig. 2(b)]. The ratio I/I_0, where I is the specular peak signal for a given coverage and I_0 is the specular peak signal for the clean surface, will be referred to as the specular reflectivity. The work function decreases to a minimum value of around $\Delta\Phi\sim-2.5$ eV at a coverage of $\Theta_{Na}\sim0.20$, before rising to a value of $\Delta\Phi\sim-2.2$ eV at completion of the monolayer at $\Theta_{Na}=0.50$. The helium reflectivity curve decreases sharply, with an increasing slope on the logarithmic scale, for sodium coverages up to approximately $\Theta_{Na}\sim0.12$. Following a reflectivity minimum of $I/I_0\approx4.5\times10^{-3}$, the reflectivity shows at least four distinct maxima at $\Theta_{Na}\sim0.125$, ~0.17, ~0.25, and ~0.50, in addition to a shoulder at $\Theta_{Na}\sim0.375$. Just as the maximum at $\Theta_{Na}=0.50$ results from the increase in specular scattering on completion of the $c(2\times2)$ layer, so do the other maxima indicate additional ordered structures. The initial slope of the reflectivity curve corresponds to a total scattering cross section[17] of $\sigma_{Na}=120$ Å^2, which is similar to the corresponding cross-sections observed for CO/Pt(111) (Ref. 17) and C_2H_4/Cu(001),[23] both of which are chemisorbed with no reconstruction of the substrate surface.

B. Time-of-flight spectra

Figure 3 shows a series of time-of-flight (TOF) spectra as a function of increasing sodium coverage at a surface temperature of $T_s=50$ K. The TOF spectrum of the clean surface shows inelastic peaks at $\Delta E\approx+9$ and $+10$ meV, which correspond to the surface Rayleigh wave and longitudinal resonance of Cu(001), respectively.[20,22] With the addition of a small quantity ($\Theta_{Na}=0.048$) of sodium, the surface phonons are almost completely suppressed, and inelastic peaks are observed at $\Delta E\approx\pm6$ meV. Inelastic measurements at different angles of incidence showed no dispersion of this vibrational mode. A similar peak at $\Delta E=5.6$ meV was observed in the HAS experiments at $T_s=180$ K by Ellis and Toennies, who assigned it to the T mode.[13] The higher frequency of $\hbar\omega=5.9$ meV at $T_s=50$ K observed here is due to the large anharmonicity of this mode, which has recently been reported.[24] With the addition of further sodium to $\Theta_{Na}=0.125$, the T-mode peak shifts to a higher frequency of $\hbar\omega=6.3$ meV. The details of the remarkable coverage-dependent frequency shifts will be discussed elsewhere.[25] At a coverage of $\Theta_{Na}=0.28$, the T-mode creation peak ($-\Delta E$) disappears, and inelastic peaks appear at a frequencies of approximately $\Delta E\approx\pm2$ meV. As for the peak at $\Delta E\approx\pm6$ meV, inelastic measurements at different angles of incidence show no dispersion of this vibrational mode. In addition, at $\Theta_{Na}=0.28$ a peak appears at $\Delta E\approx9$ meV which lies at the same position as the surface Rayleigh wave. At a higher sodium coverage of $\Theta_{Na}=0.350$, the inelastic peaks at $\Delta E=\pm2$ meV become sharper and the other inelastic peaks

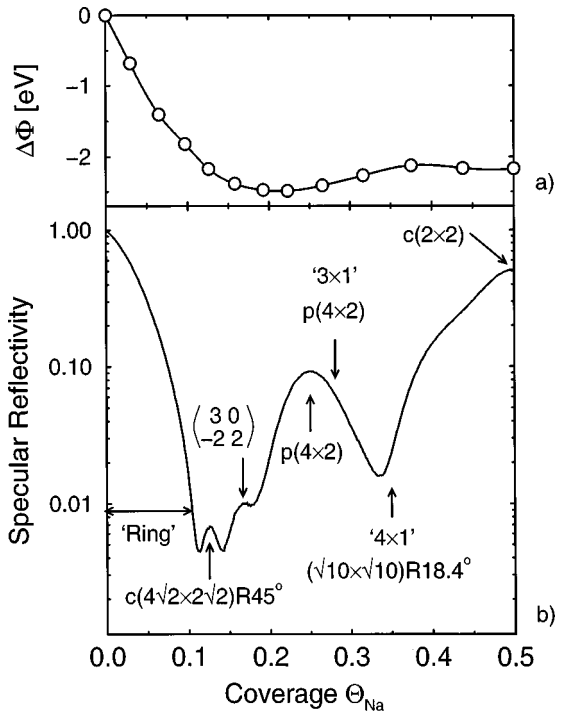

FIG. 2. (a) Comparison of the reported change of the work function at $T_s=180$ K (Ref. 11) and (b) the helium specular reflectivity as a function of sodium coverage on Cu(001) for a surface temperature of $T_s=40$ K. Note that the reflectivity is plotted on a logarithmic scale. The incident beam was directed along the [100] azimuth at an energy of 11.7 meV ($k_i=4.73$ Å^{-1}). The specular reflectivity shows several local maxima at submonolayer coverages of $\Theta_{Na}=0.125$, $\Theta_{Na}=0.17$, and $\Theta_{Na}=0.25$, as well as the maximum for the monolayer at $\Theta_{Na}=0.50$. The arrows show the coverages of the diffraction measurements reported in the present study.

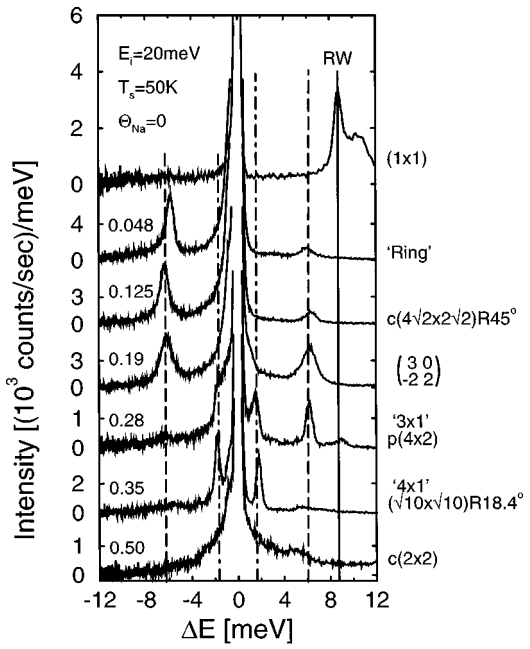

FIG. 3. Time-of-flight spectra for several different sodium coverages on Cu(001) at a surface temperature of $T_s = 50$ K. The incident He beam was directed along the [100] azimuth at an incident angle of $\theta_i = 57.9°$, which, at an incident energy of 20 meV ($k_i = 6.19$ Å^{-1}), corresponds to a parallel momentum transfer of $\Delta K = -1.43$ Å^{-1} for the elastic peak. On the clean surface the annihilation peak at $\Delta E \sim +9$ meV corresponds to the Cu(001) Rayleigh wave. Inelastic peaks due to sodium are observed at $\Delta E \sim \pm 6$ meV up to a coverage of $\Theta_{Na} \approx 0.2$, and at $\Delta E \sim \pm 2$ meV for coverages of $\Theta_{Na} > 0.2$ as indicated by the dashed vertical lines. There is no longer any evidence of sharp inelastic peaks on completion of the $c(2\times2)$ monolayer ($\Theta_{Na} = 0.50$). The diffraction pattern approximately corresponding to each TOF measurement is shown to the right of each spectrum.

at $\Delta E = \pm 6$ meV and the peak at $\Delta E = +9$ meV disappear once more. At the completion of the monolayer only a broad, weak inelastic peak at $\Delta E \approx \pm 5$ meV survives.

The presence of only one sharp inelastic peak at $\Delta E \approx \pm 6$ meV for low sodium coverages ($\Theta_{Na} < 0.2$), without an observable increase in peak width with coverage, suggests that the sodium atoms occupy equivalent sites on the surface in this coverage range. LEED I-V measurements of the $c(2\times2)$ monolayer structure for sodium on Cu(001),[11] and other alkali-metal–fcc(001) adsorption systems,[2] show that a fourfold hollow site is preferred for the monolayer. Recent molecular-dynamics simulations also indicate that sodium occupies fourfold hollow adsorption sites on Cu(001) at low coverage ($\Theta_{Na} \lesssim 0.2$).[8,26,27] Therefore, at low sodium coverages, the observed T-mode frequency of $\hbar\omega \approx 6$ meV can be related exclusively to parallel vibrations within fourfold adsorption sites. It is also worthwhile remembering at this point that $\Theta_{Na} \lesssim 0.2$ corresponds to the coverage range where the work function is decreasing, an effect which was previously related to ionic or strongly hybridized sodium atom bonding.[2,4,5]

The appearance of a second vibrational frequency at $\Delta E \approx \pm 2$ meV for $\Theta_{Na} \gtrsim 0.2$, which then almost completely replaces the 6 meV peak at $\Theta_{Na} = 0.35$ and disappears at $\Theta_{Na} = 0.50$, is of particular interest. One possible explanation for the sudden frequency decrease is that the strength of the lateral sodium-surface interaction is greatly reduced, for instance due to a sharp weakening of the sodium copper bond. The first observation of this peak coincides with the minimum and subsequent increase of the work function, as shown in Fig. 2. Since the increase of the work function for coverages up to completion of the first layer ($0.2 \lesssim \Theta_{Na} \leqslant 0.5$) has been related previously to a metalization of the alkali-metal layer; this suggests that the lowering of the T-mode frequency to $\Delta E \approx \pm 2$ meV is due to a transition from ionic to metallic bonding of sodium atoms to the surface.

An alternative explanation for the significant lowering of the T-mode frequency is a change of adsorption site from the fourfold hollow site to, for instance, the on-top site, as observed for Cs, Rb, and K on Al(111) and Cu(111).[2] However, we believe this to be unlikely since, even at completion of the monolayer ($\Theta_{Na} = 0.5$), the sodium atoms occupy exclusively fourfold hollow sites, as determined by LEED I-V measurements,[11] despite the strong Na-Na lateral interactions. For the larger alkali-metal atoms K and Cs, adsorbed on Cu(001), the lateral interaction is significantly stronger than for Na, and as a consequence the alkali-metal atoms always have a distinct hexagonal structure, even at the expense of having to occupy a range of adsorption sites.[16,28] In contrast, for the present case of Na/Cu(001), the monolayer structure is $c(2\times2)$, with a square rather than hexagonal arrangement of sodium atoms. Thus it would appear that the local lateral Na-Cu holding potential is stronger than the lateral Na-Na interactions, even when the atoms are very close together, suggesting that at lower coverages occupation of an adsorption site other than fourfold is unlikely.

C. Diffraction patterns

Two-dimensional helium angular distributions were measured for several sodium coverages to investigate the submonolayer structures formed at low temperatures. Each of the diffraction patterns shown here was obtained by stepping the polar angle $\Delta\theta$ in units of 0.3° from $\Delta\theta = -3°$ to $\Delta\theta = +32°$ for 35 different values of the tilt angle ϕ, between $\phi = -14°$ and $\phi = +3°$ (4095 data points in total). The total signal, measured for 0.5 s at each value of $\Delta\theta$ and ϕ, varies between 10^6 and 10^8 counts/s at the specular position ($\Delta\theta = 0$, $\phi = 0$) and as little as 1000 counts/s far away from the specular position. Most of the diffraction patterns are presented using a logarithmic gray scale to represent the total signal, so that all of the diffraction features can be seen.

Figure 4(a) shows a two-dimensional gray scale plot of the total scattered helium signal as a function of polar angle, $\Delta\theta$, and tilt angle, ϕ, for the lowest sodium coverage of $\Theta_{Na} = 0.047$. The diffraction pattern was measured at a temperature of $T_s = 50$ K following adsorption at $T_s = 200$ K. As shown in the schematic representation of the diffraction pattern (also plotted as a function of $\Delta\theta$ and ϕ), well-defined rings are observed around the specular and integral order diffraction peaks [Fig. 4(b)]. The radius of these rings varied with sodium coverage up to $\Theta_{Na} \sim 0.1$, with the radius increasing with the square root of the coverage, as expected. As shown in Fig. 4, the observed radius of $\Delta\theta = \pm 3.5°$ ($\Delta K = 0.50$ Å^{-1}), corresponds to an interatomic distance of

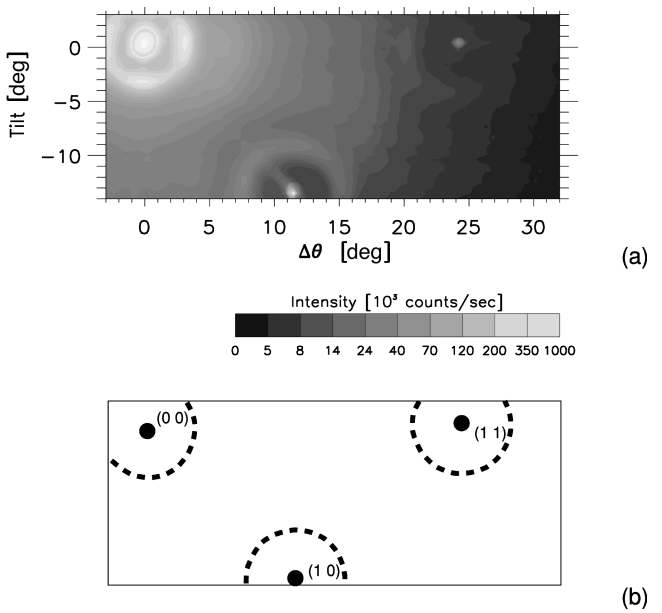

FIG. 4. (a) Two-dimensional helium angular distribution for a sodium coverage of $\Theta_{Na}=0.047$ at a surface temperature of $T_s=50$ K. The incident-beam energy was 20 meV ($k_i=6.19$ Å^{-1}). The diffraction features in (a) are shown schematically in (b). The intensity axis has been plotted on a logarithmic scale to highlight the rings around the specular and integral order diffraction peaks at $\Delta\theta=12.0°$ and $\phi=-13.5°$, and at $\Delta\theta=24.2°$ and $\phi=0°$. The diffraction rings have a radius of $\Delta K=0.50$ Å^{-1} which corresponds to an average Na-Na separation of 12.6 Å.

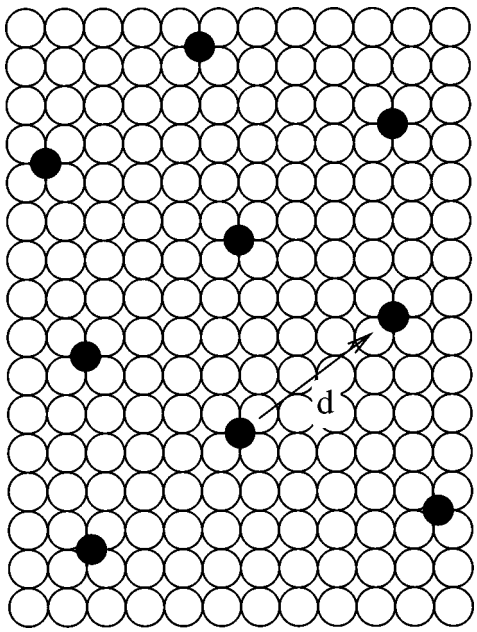

FIG. 5. Schematic diagram of the arrangement of sodium atoms as deduced from the diffraction pattern measured for $\Theta_{Na}\sim0.047$ shown in Fig. 4. The repulsion between the sodium atoms is minimized by the near-hexagonal structure in which the interatomic distance d between the atoms is nearly the same. The observed diffraction peaks are smeared into a ring by the azimuthal rotation of consecutive domains of quasihexagonal structure.

12.6 Å. Some variation of the diffraction ring intensity with azimuth can be seen, particularly for the ring around the specular peak. The ring intensity appears to be largest along the [100] and [010] azimuths, while it is lower along the [110] and [1$\bar{1}$0] azimuths. The origin of the intensity variation could lie either in a slightly greater probability of having domains aligned close to the [100] and [010] azimuths when compared to other azimuths, or in a slight asymmetry of the scattering form factor from isolated sodium atoms due to the presence of the Cu(001) surface.

Similar diffraction ring structures have been observed with LEED for many different alkali metals on various low-index metal surfaces.[2] These structures are generally attributed to slightly disordered hexagons arising from the repulsion between adsorbed alkali-metal atoms, which are smeared into a ring by the azimuthal rotation of consecutive domains. This interpretation is consistent with the observed coverage dependence of the ring diameter.[16] The observation of the T-mode frequency at $\hbar\omega\approx6$ meV in the inelastic measurements (Fig. 3) which, as discussed in Sec. III B, has been assigned to parallel vibrations at the fourfold hollow sites, indicates that all of the sodium atoms occupy the same fourfold hollow sites on Cu(001). An approximate model of a sodium atom overlayer with $\Theta_{Na}\sim0.047$, based on these ideas, is shown schematically in Fig. 5.

Diffraction patterns similar to that shown in Fig. 4 were observed up to about $\Theta_{Na}\sim0.1$. At $\Theta_{Na}=0.125$, which corresponds to the first maximum of the reflectivity curve (Fig. 2), a more complex arrangement of diffraction peaks, as shown in Fig. 6(a), is observed, again measured at $T_s=50$ K following adsorption at $T_s=200$ K. The diffraction peak positions can now be described by two domains of a $c(4\sqrt{2}\times2\sqrt{2})R45°$ overlayer structure which are rotated by 90° with respect to each other. The reciprocal space unit cell for the two domains is shown schematically in Fig. 6(b). A similar $c(4\sqrt{2}\times2\sqrt{2})R45°$ overlayer structure was observed in LEED patterns for $\Theta=0.125$ caesium adsorbed on Rh(001) by Müller, Besold, and Heinz,[3] and for potassium on Ni(001) by Wedler *et al.*[29] Since at this coverage the same T-mode frequency as found at lower coverages was measured (Fig. 3), the sodium atoms again appear to occupy the same hollow sites. A $c(4\sqrt{2}\times2\sqrt{2})R45°$ structure consistent with these sites is shown in Fig. 7. It is interesting to note that, on heating to $T_s=100$ K, the sharp diffraction peaks visible at $T_s=50$ K in Fig. 6 gradually disappear. This is attributed to rapid diffusion of the sodium atoms even at these low temperatures, which is facilitated by the low diffusion barrier of $E_{diff}=51\pm6$ meV.[13]

Further adsorption of sodium to a slightly higher coverage of $\Theta_{Na}=0.16$, close to the second maximum of the reflectivity curve at $\Theta_{Na}=0.17$, leads to a subtle change of the diffraction pattern from the $c(2\sqrt{2}\times4\sqrt{2})R45°$ arrangement observed at $\Theta_{Na}=0.125$. The $(\frac{3}{8}\ \frac{1}{8})$ peaks merge to form a broad peak at $(\frac{1}{3}\ 0)$, as shown in Fig. 8. The peak maxima can be described now by reciprocal-lattice vectors corresponding to the $(\frac{1}{3}\ 0)$ and $(\frac{1}{4}\ \frac{1}{4})$ diffraction peak positions, i.e., $\begin{pmatrix}3 & 0\\ -2 & 2\end{pmatrix}$. The corresponding ideal structure with a coverage of $\Theta_{Na}=0.167$ is shown in Fig. 9. The broadness of the diffraction peaks observed indicates a significant degree of disorder even at $T_s=50$ K. The substantial broadening of the $(\frac{1}{3}\ 0)$ peaks perpendicular to the [110] azimuth indicates a significant variation in the angle of the $\begin{pmatrix}3\\ -2\end{pmatrix}$ superstructure

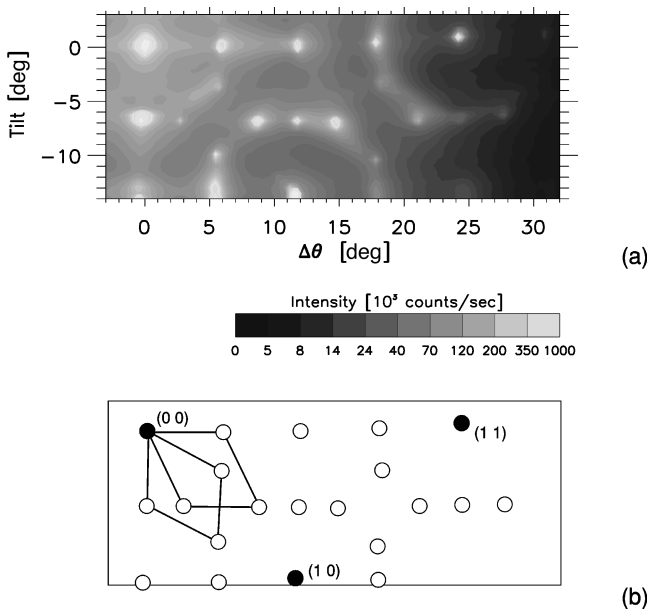

FIG. 6. (a) Two-dimensional helium angular distribution for a sodium coverage of $\Theta_{\mathrm{Na}}=0.125$ at a surface temperature of $T_s=50$ K. The incident-beam energy was 20 meV ($k_i=6.19$ Å^{-1}). The intensity axis was plotted on a logarithmic gray scale to highlight the diffraction peaks from the sodium overlayer structure. The diffraction peaks in (a) are shown schematically in (b). With the exception of the Cu(001) diffraction peaks, marked by filled circles, the peaks marked by open circles correspond to two domains of a $c(4\sqrt{2}\times 2\sqrt{2})R45°$ sodium superstructure, for which the unit cells are shown in (b).

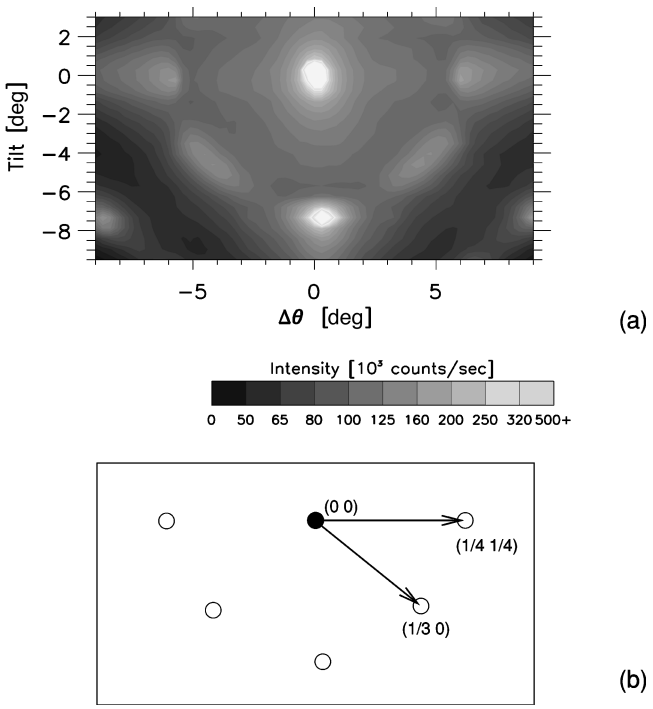

FIG. 8. (a) Two-dimensional helium angular distribution for a sodium coverage of $\Theta_{\mathrm{Na}}=0.16$ at a surface temperature of $T_s=50$ K. The incident-beam energy was 20 meV ($k_i=6.19$ Å^{-1}). The intensity axis was plotted on a logarithmic gray scale to highlight the diffraction peaks in a small section of reciprocal space surrounding the specular peak. The diffraction peaks and lattice vectors are shown schematically in (b), and correspond to a $\begin{pmatrix} 3 & 0 \\ -2 & 2 \end{pmatrix}$ sodium superstructure.

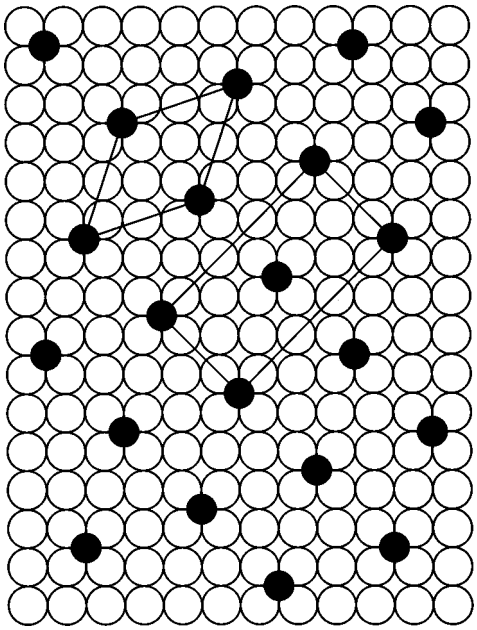

FIG. 7. Schematic diagram showing a section of one domain of the $c(2\sqrt{2}\times 4\sqrt{2})R45°$ structure as deduced from the diffraction pattern measured for $\Theta_{\mathrm{Na}}=0.125$ shown in Fig. 6. In this structure there are two sodium-sodium distances of 7.22 and 8.07 Å.

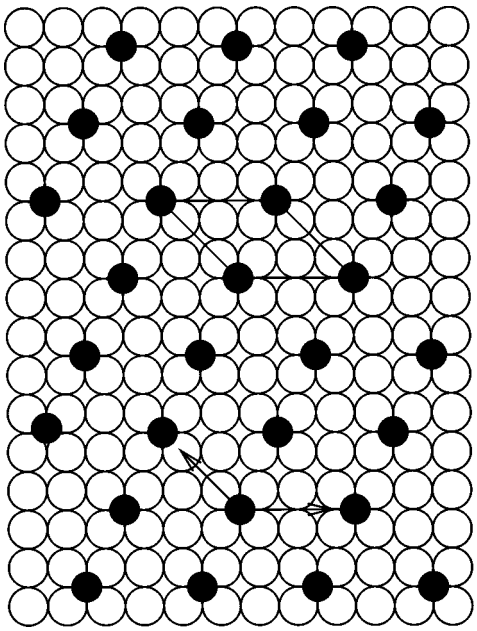

FIG. 9. Schematic diagram showing a section of one domain of the approximate arrangement of the $\begin{pmatrix} 3 & 0 \\ -2 & 2 \end{pmatrix}$ structure as deduced from the diffraction pattern measured for $\Theta_{\mathrm{Na}}=0.16$ shown in Fig. 8. In this structure there are three sodium-sodium distances of 7.22, 5.72, and 7.67 Å.

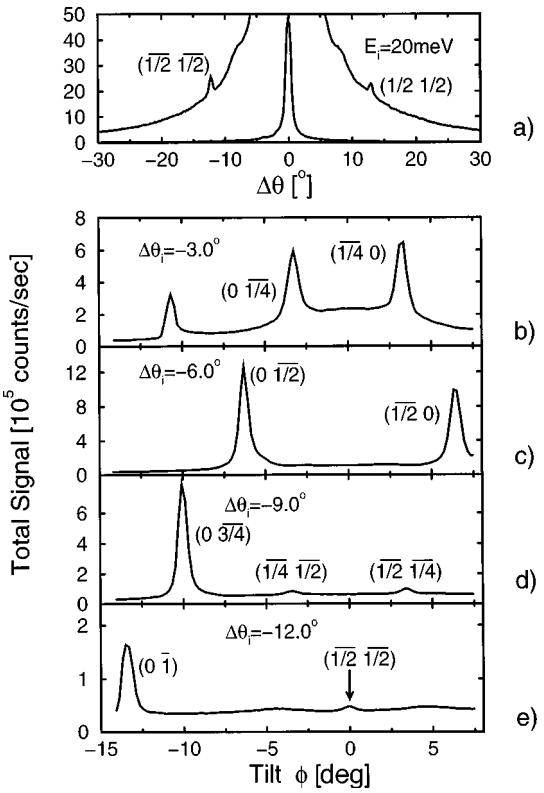

FIG. 10. A series of helium angular distributions obtained by rotating the polar angle and tilting the surface for a sodium coverage of $\Theta_{Na}=0.25$ at a surface temperature of $T_s=50$ K. The incident-beam energy was 20 meV ($k_i=6.19$ Å^{-1}). Intense peaks at $(0\ \frac{1}{4})$, $(0\ \frac{1}{2})$, $(0\ \frac{3}{4})$, $(\frac{1}{4}\ 0)$, and $(\frac{1}{2}\ 0)$, and weaker peaks at $(\frac{1}{4}\ \frac{1}{2})$ and $(\frac{1}{2}\ \frac{1}{2})$, correspond to diffraction from a $p(4\times2)$ sodium overlayer. The peak at $\Delta\theta=-12.0°$ and $\phi=-13.0°$ corresponds to a Cu(001) diffraction position.

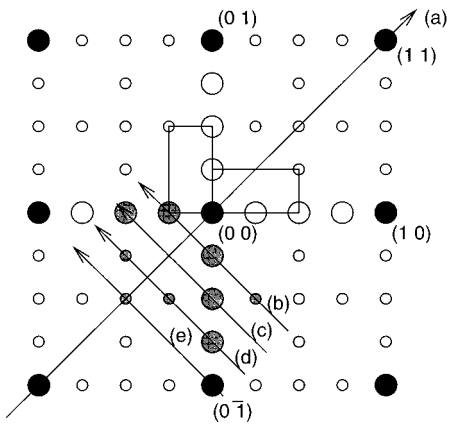

FIG. 11. Schematic diagram showing the positions of the diffraction peaks of Fig. 10 in reciprocal space for $\Theta_{Na}=0.25$. The integer order Cu(001) diffraction positions are indicated by the completely filled circles (●). The shaded circles with the arrows $(a)-(e)$ indicate the peaks and the direction of the corresponding angular distributions in Fig. 10 with the more intense peaks shown by large shaded circles. The $p(4\times2)$ diffraction pattern is completed for all four quadrants by the open circles (○), and the reciprocal space unit cell is shown for the two orthogonal domains.

lattice vector with respect to the [110] azimuth. This disorder is perhaps not so surprising, considering the significant difference between the three competing sodium-sodium distances of 5.72, 7.22, and 7.67 Å.

At a coverage of $\Theta_{Na}=0.25$, the third, and most intense, submonolayer maximum of the reflectivity curve is found (see Fig. 2). At this coverage an entirely different set of diffraction peak positions are observed, as shown by the series of angular distributions in Fig. 10. These scans are shown rather than the 2D gray scale plots presented up to now in order to highlight the distribution of intensity between the various diffraction peaks. Figure 10(a) shows an angular distribution obtained by rotating the polar angle $\Delta\theta$ along the Cu(001) [100] azimuth, through the (1 1), (0 0), and (1 1) Cu(001) diffraction peak positions. Figures 10(b)–10(e) are selected tilt angular distributions along the [010] azimuth through the $(\frac{1}{8}\ \frac{1}{8})$, $(\frac{1}{4}\ \frac{1}{4})$, $(\frac{3}{8}\ \frac{3}{8})$, and $(\frac{1}{2}\ \frac{1}{2})$ diffraction peak positions, respectively. The well-defined diffraction peaks correspond to two orthogonal domains of a $p(4\times2)$ structure shown in Fig. 11.

The most intense diffraction peaks were observed in the quarter-order diffraction positions $(\frac{1}{4}\ 0)$, $(\frac{1}{2}\ 0)$, and $(\frac{3}{4}\ 0)$ along the Cu(001) [110] and [110] azimuths. The only way to obtain intense diffraction peaks almost exclusively along only the [110] and [110] azimuths is to have two orthogonal domains of a surface structure, each domain of which is strongly corrugated along only one of these azimuthal directions. If an overlayer unit cell with a more complex 2D corrugation with significant components along more than just one azimuthal direction were present, then large intensities would be observed in all of the diffraction peaks and not just those located along particular azimuths. Consequently, the diffraction intensities suggest that the sodium atoms form two orthogonal domains of a quasi-one-dimensional structure oriented along the [110] and [110] azimuths, as shown in Fig. 12. In this structure the sodium atoms are arranged in rows along the [100] and [110] azimuths spaced $4a$ apart (see Fig. 12), with a local $c(2\times2)$ structure. The large $4a$ spacing between the rows gives a strong corrugation which leads to the large helium atom diffraction intensity along the [110] and [110] azimuths. The low diffraction intensity away from the [110] and [110] azimuths at this coverage indicates the absence of significant corrugation along the sodium atom rows. Such a low corrugation is incompatible with the corrugation anticipated for well-separated, ionically surface bonded sodium atoms, such as those forming the $c(4\sqrt{2}\times2\sqrt{2})R45°$ structure at a lower coverage of $\Theta_{Na}=0.125$. In that case, significant diffraction intensity was observed in all azimuthal directions. Thus, the one-dimensional character of the diffraction peak intensity distribution strongly suggests a smoothing of the corrugation along the sodium atoms rows. This interpretation is consistent with the work-function data, shown in Fig. 2, which suggest that the sodium rows have a considerable metallic character which would also tend to smooth out the corrugation along the rows.

With only a small further increase of the sodium coverage from $\Theta_{Na}=0.25$ to $\Theta_{Na}=0.28$, the helium diffraction pattern changes significantly to that shown in Fig. 13. The most intense diffraction peaks are again oriented along the Cu(001) [110] and [110] azimuths, as also observed for $\Theta_{Na}=0.25$. In this case, however, the diffraction peaks are broadened along the [110] and [110] azimuths, respectively,

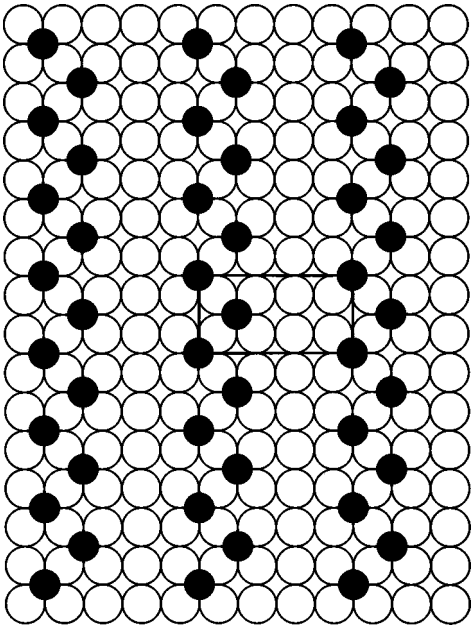

FIG. 12. Proposed structure for a sodium coverage of $\Theta_{Na}=0.25$ determined from the $p(4\times2)$ diffraction pattern shown in Fig. 10. The sodium atoms form quasi-one-dimensional rows which provide for a strong corrugation along the [110] and [1$\bar{1}$0] azimuths for the two orthogonal domains.

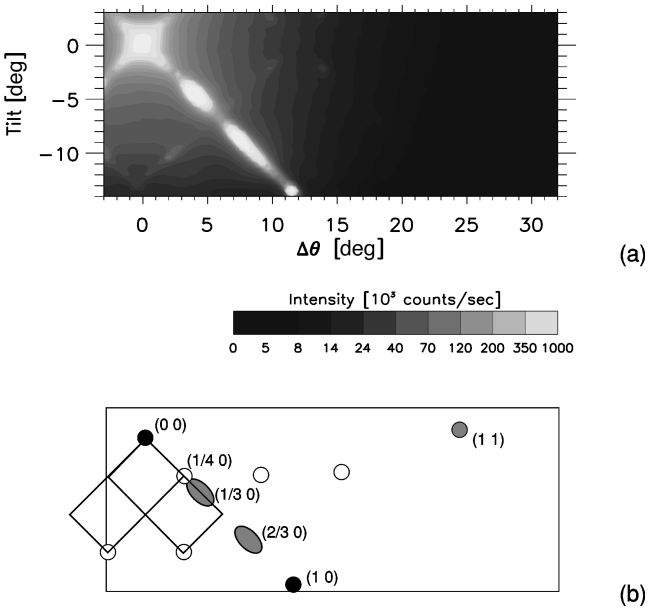

FIG. 13. Two-dimensional helium angular distribution for a sodium coverage of $\Theta_{Na}=0.28$ at a surface temperature of $T_s=50$ K. The incident-beam energy was 20 meV ($k_i=6.19$ Å^{-1}). The intensity was plotted on a logarithmic gray scale to highlight the intense diffraction peaks observed at approximately the ($\frac{1}{3}$ 0) and ($\frac{2}{3}$ 0) diffraction positions which are broadened significantly along the Cu(001) [110] azimuth. The filled circles in (b) mark the diffraction positions of the Cu(001) surface. Additional, weak diffraction peaks are found in positions corresponding to a $p(4\times2)$ pattern.

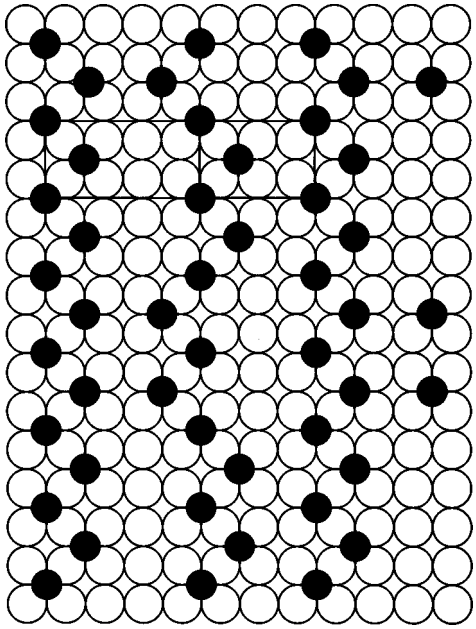

FIG. 14. Schematic diagram showing a proposed arrangement of sodium atoms for $\Theta_{Na}=0.28$. Kinks have been introduced into alternate rows to accommodate the additional sodium atoms. This mixture of 4×2 and 3×2 unit cells shown in the arrangement leads to additional intense, broad diffraction peaks between the quarter- and third-order diffraction positions along the [110] and [1$\bar{1}$0] azimuths (see Fig. 13).

corresponding to a distribution of unit-cell lengths between $3a$ and $4a$. Some low-intensity $p(4\times2)$ diffraction peaks can still be observed. The relatively small increase in coverage from $\Theta_{Na}=0.25$ to $\Theta_{Na}=0.28$, and the diffraction peak intensity distribution, suggest that the overlayer structure at $\Theta_{Na}=0.28$ is probably a modified version of the $p(4\times2)$ structure, with kinks in the sodium atom rows to accommodate the additional atoms. Figure 14 shows a schematic diagram of this proposed structure.

Figure 15(a) shows a two-dimensional helium angular distribution obtained for a sodium coverage of $\Theta_{Na}=0.350$. As for $\Theta_{Na}=0.25$ and 0.28, this angular distribution shows strong quarter-order diffraction peaks along the [110] and [1$\bar{1}$0] azimuths, again suggesting that the sodium atoms form predominantly one-dimensional structures on the surface, also with $4a$ periodicity. Additional, weaker, diffraction peaks corresponding to two domains of a $(\sqrt{10}\times\sqrt{10})R18.4°$ structure are observed, as shown by the reciprocal unit cells in the schematic representation of the diffraction pattern in Fig. 15(b). The large intensity difference between the strong 4×1 diffraction peaks and the weaker $(\sqrt{10}\times\sqrt{10})R18.4°$ diffraction peaks strongly suggests that the surface is composed of a mixture of domains of these two different structures, with different sodium coverages which contribute to the average sodium coverage of $\Theta_{Na}=0.350$. The ideal coverages of these two phases depends on the possible structures which will be discussed next.

One possible overlayer structure which is consistent with the large diffraction intensities of the quarter-order diffraction peaks along the [110] and [1$\bar{1}$0] azimuths is shown in Fig. 16. This structure is similar to the row structure proposed in Fig. 12 for a sodium coverage of $\Theta_{Na}=0.25$, only

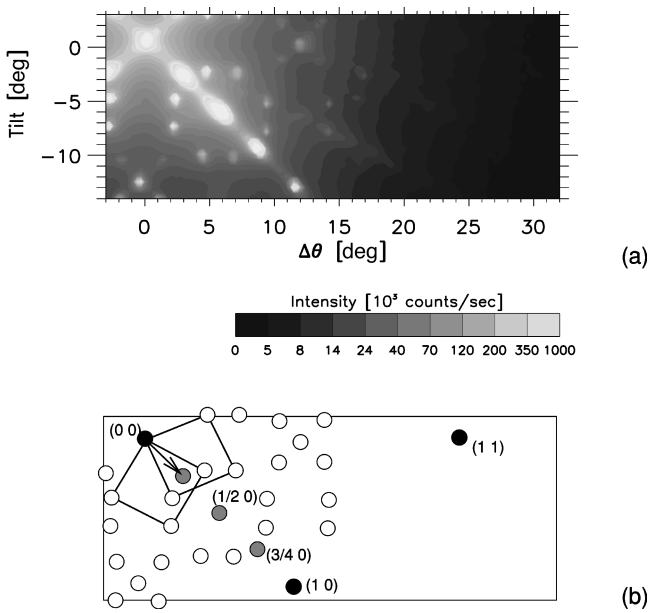

FIG. 15. Two-dimensional helium angular distribution for a sodium coverage of $\Theta_{Na}=0.350$ at a surface temperature of $T_s=50$ K. The incident-beam energy was 20 meV ($k_i=6.19$ Å^{-1}). The intensity was plotted on a logarithmic gray scale to highlight the diffraction peaks. Intense overlayer diffraction peaks, marked by gray circles, are observed at the ($\frac{1}{4}$ 0), ($\frac{1}{2}$ 0), and ($\frac{3}{4}$ 0) diffraction positions, while the filled circles in (b) mark diffraction positions of the Cu(001) surface. Additional, sharp, but less intense diffraction peaks, marked by open circles, indicate diffraction positions corresponding to a $(\sqrt{10}\times\sqrt{10})R18.4°$ overlayer, for which the unit cells for two domains are also shown.

with the addition of an extra string of sodium atoms within each row to increase the coverage to $\Theta_{Na}=0.375$. The shoulder observed in the specular reflectivity curve in Fig. 2 at $\Theta_{Na}=0.375$ supports this interpretation and the existence of a well-defined structure in the coverage range $\Theta_{Na}\sim 0.350-0.400$. As already discussed for $\Theta_{Na}=0.25$ and 0.28, the one-dimensional character of this structure provides for a strong surface corrugation perpendicular to the sodium atom rows resulting in higher diffraction intensities along the [110] ([$\bar{1}$10]) azimuth.

The coverage of this structure of $\Theta_{Na}=0.375$ is somewhat larger than the experimental coverage of $\Theta_{Na}=0.350$ so, to compensate, the structure corresponding to the $(\sqrt{10}\times\sqrt{10})R18.4°$ diffraction peaks must have a coverage which is less than $\Theta_{Na}=0.35$. Figure 17 shows a section of one domain of a possible structure with the correct $(\sqrt{10}\times\sqrt{10})R18.4°$ unit cell which has a coverage of $\Theta_{Na}=0.30$. In this $(\sqrt{10}\times\sqrt{10})R18.4°$ structure, the sodium atoms are situated in $c(2\times2)$ positions on the surface which form rows similar to the proposed structures for $\Theta_{Na}=0.25$ and 0.375. This structure also follows from the structure proposed for $\Theta_{Na}=0.28$, only with an ordered array of kinks with one orientation. The net effect of this is to maximize the distance between the rows while increasing the coverage from that of the $p(2\times4)$ structure proposed for $\Theta_{Na}=0.25$ (Fig. 12).

It is interesting to note that the structure in Fig. 16 is also consistent with the $c(2\times2)$ diffraction pattern reported for

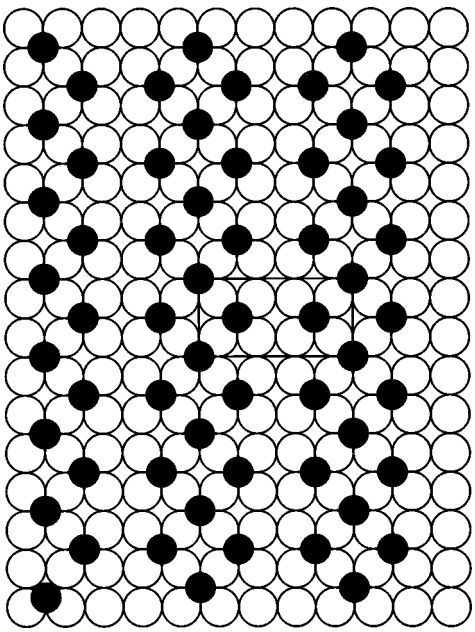

FIG. 16. A section of one domain of a sodium overlayer structure model suggested by the intense 4×1 diffraction peaks observed in Fig. 15. The sodium coverage of this structure is $\Theta_{Na}=0.375$, close to the value of $\Theta_{Na}=0.350$ measured in Fig. 15. The one-dimensional character of this overlayer structure gives a strong surface corrugation along the [110] and [$\bar{1}$10] azimuths, leading to the observation of intense diffraction peaks along those azimuths.

$T_s=180$ K using LEED at the same coverage.[11] These results suggest that the sodium atoms organize into a $c(2\times2)$ arrangement of sodium atoms, even though the monolayer is not yet complete. For this reason the sodium atoms

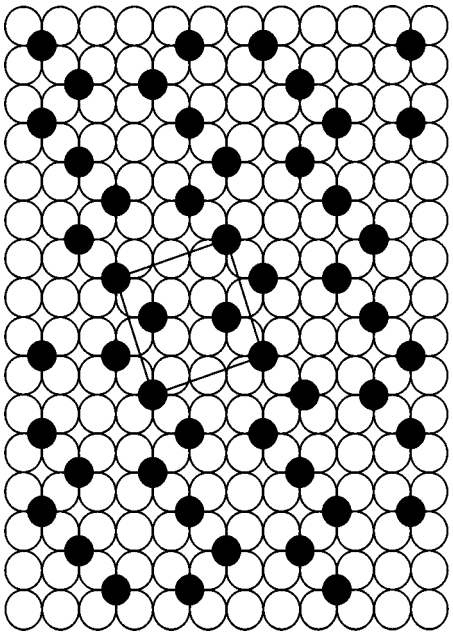

FIG. 17. One possible $(\sqrt{10}\times\sqrt{10})R18.4°$ sodium overlayer structure to explain the weak diffraction peaks observed for a sodium coverage of $\Theta_{Na}=0.350$ shown in Fig. 15. The sodium coverage is $\Theta_{Na}=0.30$, and follows the trend of the quasi-one-dimensional structures which sodium forms at coverages of $\Theta_{Na}=0.25$ and above.

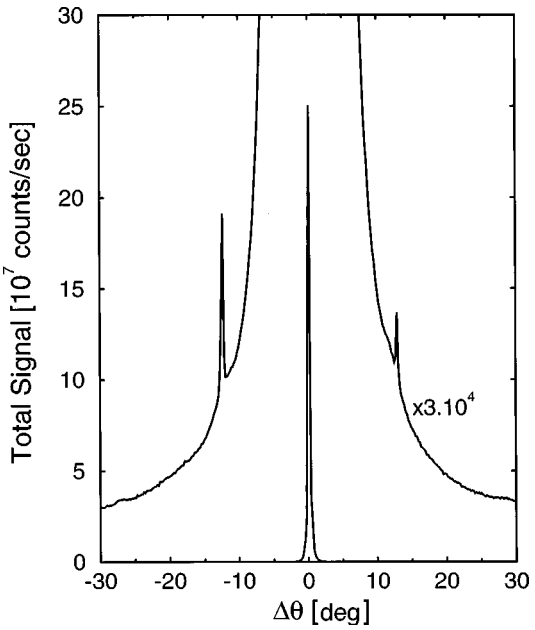

FIG. 18. Angular distribution for a sodium coverage of $\Theta_{Na}=0.50$ at a surface temperature of $T_s=50$ K. The incident-beam energy was 20 meV ($k_i=6.19$ Å^{-1}) oriented along the Cu(001) [100] azimuth. Low-intensity, sharp, diffraction peaks are observed at $\Delta\theta=\pm 12°$, corresponding to the $(\frac{1}{2}\ \frac{1}{2})$ diffraction positions at $\Delta K=\pm 1.74$ Å^{-1}, in addition to the intense specular peak. The apparent intensity difference between the two $(\frac{1}{2}\ \frac{1}{2})$ diffraction peaks is probably due to a small misalignment of the crystal azimuth.

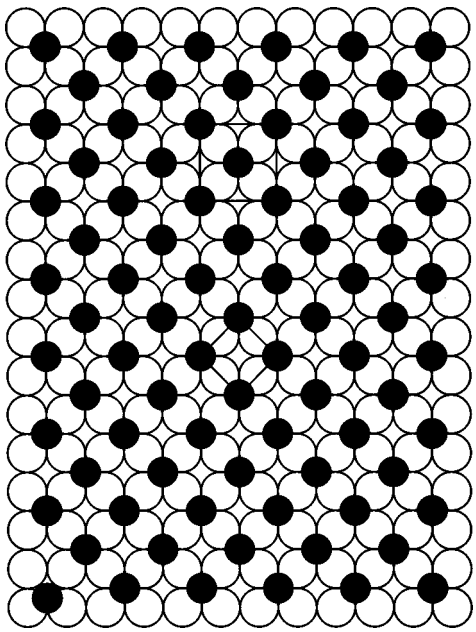

FIG. 19. Schematic diagram showing the sodium atom positions for the $c(2\times 2)$ structure observed for $\Theta_{Na}=0.500$ (Fig. 18). LEED I-V measurements suggest that the sodium atoms sit in fourfold hollow sites at this coverage (Ref. 11).

are shown in next-nearest-neighbor fourfold hollow sites in a local $c(2\times 2)$ arrangement within the rows, even though the helium diffraction data do not provide information on the internal structure of the rows due to the lack of corrugation along the rows.

Following completion of the sodium monolayer, as determined from the near-unity normalized specular reflectivity (Fig. 2),[17] the polar angle angular distribution shown in Fig. 18 was measured along the Cu(001) [100] azimuth. The observed $(\frac{1}{2}\ \frac{1}{2})$ diffraction peaks are very sharp, indicating a high degree of order in the overlayer. Their very low intensity which, on average, is approximately 10^{-5} of the specular peak, indicates that the surface is very smooth, in fact about as smooth as the clean Cu(001) surface.[30] Such a smooth corrugation is anticipated for a metallic layer, where the valence electrons provide a Smoluchowski smoothing of the corrugation formed by the ion cores. Thus the low corrugation is consistent with a strong metallic character of the sodium monolayer.

In Fig. 19 a schematic diagram showing the arrangement of sodium atoms in the $c(2\times 2)$ overlayer is shown. A $c(2\times 2)$ diffraction pattern has also been observed using low-energy electron diffraction for sodium adsorbed on Cu(001) (Ref. 11) and Ni(001).[31] As mentioned earlier, LEED I-V analysis has shown that, on Cu(001) surfaces, sodium atoms occupy fourfold hollow sites.[11]

IV. DISCUSSION

These new helium diffraction results show that sodium exhibits a rich variety of overlayer structures on Cu(001) at low temperatures. The present helium diffraction results obtained following adsorption at a temperature of $T_s=200$ K and measurement at $T_s=50$ K are summarized and compared with those obtained using LEED at a higher temperature of $T_s=180$ K (Ref. 11) in Table II. In addition to the diffraction results obtained for a temperature of $T_s=50$ K, some HAS results measured at a temperature of $T_s=100$ K, which were also obtained during the present study, are indicated. The helium diffraction and electron-diffraction results are in good agreement in the low coverage regime, $\Theta_{Na}\lesssim 0.2$, taking into account the fact that the high diffusion rate at $T_s=180$ K (Ref. 13) breaks up the long-range order of the overlayer structures which could be observed here at lower temperatures. The low-coverage surface structure is dominated by repulsive dipolar interactions leading to a series of quasihexagonal structures for which the local order is strongly temperature dependent. At $\Theta_{Na}=0.125$, a $c(4\sqrt{2}\times 2\sqrt{2})R45°$ structure was observed, as expected from a consideration of the competition between the lateral photoemission spectroscopy and purely repulsive alkali-metal–alkali-metal interactions.[8,32]

The helium diffraction results confirm that the monolayer structure is $c(2\times 2)$, as observed using LEED.[11] Unlike the larger alkali-metal atoms,[1,16] which form hexagonal overlayer structures at completion of the monolayer, sodium atoms adsorbed on Cu(001) form a square lattice, indicating that the local lateral bonding dominates in the determination of the equilibrium adsorption site. This site was determined to be fourfold hollow,[11] in common with Li/Cu(001) (Ref. 11) and Na/Ni(001).[1]

In the intermediate submonolayer coverage regime the present results differ, substantially, from both the reported LEED results at higher temperatures, and theoretical expectations, since the diffraction patterns observed here for $\Theta_{Na}=0.25$, 0.28, and 0.35 have not been observed previously, to

TABLE II. Comparison of the submonolayer structures of sodium atoms adsorbed on Cu(001) determined in the present study using helium-atom scattering (HAS) at $T_s = 50$ and 100 K with a low-energy electron-diffraction (LEED) study at $T_s = 180$ K (Ref. 11).

Coverage Θ_{Na}	HAS $T_s = 50$ K	HAS $T_s = 100$ K	LEED $T_s = 180$ K (Ref. 11)
<0.1	Ring	Weak ring	Ring
0.125	$c(4\sqrt{2}\times 2\sqrt{2})R45°$	Weak ring	Ring
0.167	$\begin{pmatrix} 3 & 0 \\ -2 & 2 \end{pmatrix}$		Ring
0.25	$p(4\times 2)$		Ring
0.28	3×1 $p(4\times 2)$	3×1	$c(14\times 2)$ hex
0.30	$(\sqrt{10}\times\sqrt{10})R18.4°$	$(\sqrt{10}\times\sqrt{10})R18.4°$	$c(14\times 2)$ hex
0.375	4×1	4×1	$c(2\times 2)$
0.50	$c(2\times 2)$	$c(2\times 2)$	$c(2\times 2)$

our knowledge, for the adsorption of any alkali metal on a fcc(001) metal surface. For an unspecified alkali metal at a coverage of $\Theta = 0.25$ on a fcc(001) surface, an overlayer of $c(4\times 2)$ structure was calculated in Ref. 32. In this $c(4\times 2)$ structure, which had been observed previously for Cs/Rh(001) (Ref. 3) and K/Ni(001),[33] the alkali-metal atoms form a quasihexagonal structure due to dipolar repulsion. However, the present results show that, at the same coverage, the sodium atoms form a $p(4\times 2)$ overlayer structure on Cu(001). Moreover, the distribution of diffraction intensities indicates that the structure is essentially one dimensional in nature, suggesting a condensation of the sodium atoms into metallic rows. A quasi-one-dimensional character was also observed at coverages of $\Theta_{Na} = 0.28$ and 0.35, indicating that this is a general preference for this particular adsorption system.

It is worthwhile noting that the diffraction results alone do not completely rule out the possibility of a one-dimensional reconstruction of the Cu(001) surface, with the sodium atoms occupying higher coordinated sites. However, there are two pieces of evidence against this possibility. First, as noted in the literature,[1,2,7] reconstruction of the surface typically only takes place at higher temperatures approaching room temperature. In particular, fcc(110) surfaces, and surfaces with adsorbed lithium, are prone to reconstruction.[2] In addition, no indication of reconstruction in this coverage and temperature range was found in the LEED investigations.[11] Second, the measured T-mode frequency, shown in Fig. 3, drops by a factor of 3 from that of the isolated atom at lower coverage, but the intensity is about the same. The lower lateral vibration frequency would appear to be incompatible with a higher sodium-atom coordination, if anything, a higher frequency and lower intensity would be anticipated. Consequently, based on this evidence, it is our opinion that the Cu(001) surface does not reconstruct, but rather than the sodium atoms themselves group to form quasi-one-dimensional structures.

Condensation of adsorbed alkali-metal atoms into islands has been observed for several other alkali-metal adsorption systems, as reviewed in detail by Diehl and McGrath.[2] They concluded that the reason why island condensation occurs for some systems and not for others is related to the balance between lateral local bond and interatomic forces. The heavier alkali metals, K, Rb, and Cs, are less likely to condense due to their dipole moment being more than twice as large as for sodium. In addition, it has been determined recently that the lateral variation of the adsorption potential decreases for the larger alkali-metal atoms.[38] Thus the conditions for island formation are particularly favorable for sodium.

As far as we are aware, there have been few reports in the literature of one-dimensional structures of alkali and alkali-earth metal atoms adsorbed on various flat surfaces [e.g., Sr/Mo(112), Li/W(112), Mg/W(112), Na/Mo(112)].[34] The asymmetric islands shapes were attributed to asymmetries in indirect electronic interactions as a result of the asymmetric structure of the metal surface for which this effect was observed. For Cu($\underline{0}01$) there are no obvious difference between the [110] and [$\bar{1}$10] azimuths which may lead to asymmetric island shapes.

The effect of a large work-function difference between an adsorbate island and substrate upon surface order was discussed by Vanderbilt and co-workers,[35,36] with particular reference to the periodic domain structure observed for the O/Cu(110) system.[37] Ng and Vanderbilt considered the energy density due to various domain structures for different adsorbate coverages where the surface can be characterized by two distinct phases with different work functions. The energy associated with the boundary of an island or atom (surface tension) competes with direct, long-range electrostatic interactions between the two phases, which results in a transition from a regular hexagonal arrangement of circular ''droplets'' (atoms) to a periodic row phase as soon as the reduction in the boundary energy arising from the formation of striped domains is greater than the corresponding increase in electrostatic energy due to the reduced distance between adsorbates.[36]

In the present case, Na/Cu(001), the two phases are the clean Cu(001) surface and the Na-covered surface, which have significantly different work functions (see Fig. 2). At the predicted transition coverage $\Theta_{Na} = 0.25$, which is half of the monolayer coverage, the sodium atoms were observed to form row structures, whereby the boundary energy is reduced considerably compared with a quasihexagonal arrangement of separate sodium atoms. For alkali-metal adsorption, in addition, the work function increases once the atoms coalesce to form metallic islands. This effect reduces the electrostatic repulsion between the atoms in the rows.

Ng and Vanderbilt further predicted that, at coverages between half of saturation and saturation [$0.25 \lesssim \Theta_{Na} \lesssim 0.5$ for Na/Cu(001)], the system should return to circularly or hexagonally shaped inverse adsorbate droplets, corresponding to holes in the adsorbate layer, but only if the substrate potential is isotropic. The relatively high value of the diffusion barrier[13] for Na/Cu(001), compared with the repulsion between the sodium atoms, means that the sodium atoms feel the anisotropy of the surface potential and, therefore, ''prefer'' fourfold hollow sites to any other adsorption site. In this case Ng and Vanderbilt predicted that the system may not return to the droplet phase following the periodic row phase at half-saturation coverage. Thus the results of their model indicated that, in the present case, sodium forms a periodic row structure on Cu(001) at $\Theta_{Na} = 0.25$ in order to minimize the strength of the electrostatic interactions between the atoms and, further, that the sodium atoms remain in a periodic row arrangement because of the relatively strong preference sodium shows for adsorption at four-fold hollow sites.

The present observations raise the question, why the same effect is not seen for other alkali metal systems? We suggest that the same relative balance between the lateral local bond and the interatomic forces which favor island formation (see above) also favor row structures. As noted above, the dipole repulsion for Na is much weaker in relation to the local bond forces than for the heavier alkali-metal atoms, e.g., K and Cs, on Cu(001). Thus, not only is island formation less favorable for K, Rb, and Cs, but, if they do form islands it is unlikely that they form row structures. Thus it would seem that the Na/Cu(001) system provides an optimum balance of interactions for the structures predicted by Ng and Vanderbilt.[36]

V. CONCLUSION

Submonolayer coverages of sodium on Cu(001) have been investigated with high-resolution helium-atom diffraction in two-dimensional reciprocal-lattice space. Inelastic time-of-flight measurements of the parallel frustrated translation (T mode) showed a substantial variation between the low-coverage regime, $\Theta_{Na} \lesssim 0.2$, and higher coverages up to completion of the monolayer, $0.25 \lesssim \Theta_{Na} \lesssim 0.50$. At low coverages the T-mode frequency is $\hbar\omega \sim 6$ meV, which changes to $\hbar\omega \sim 2$ meV at higher coverages. These trends are correlated with the helium diffraction patterns which, at low coverages, show a transition with increasing coverage from isotropic ringlike structures to asymmetric row structures along the [110] and [110] azimuths, which, at larger coverages, finally leads to the isotropic $c(2\times2)$ saturation coverage structure. For $\Theta_{Na} \lesssim 0.2$ the overlayer structures can be characterized by repulsive interactions between separate sodium atoms which reside in the same type of adsorption site (fourfold hollow) corresponding to high T-mode frequencies of $\hbar\omega \approx 6$ meV, while, at higher coverages $0.2 \lesssim \Theta_{Na} \lesssim 0.50$, the sodium atoms condense into one-dimensional islands which are most likely metallic in nature, corresponding to low T-mode frequencies of $\hbar\omega \approx 2$ meV. The present results indicate that a complex balance exists between the various interatomic interactions present and, further, that in this case, in agreement with the theory of Vanderbilt and co-workers,[35,36] the balance leads to the predicted row structures expected for an ionic adsorbate system.

ACKNOWLEDGMENTS

The authors would like to thank Dr. E. Hulpke and Professor J. R. Manson for their critical reading of this manuscript, and for many helpful discussions.

[1] R. D. Diehl and R. McGrath, Surf. Rev. Lett. **2**, 387 (1995).
[2] R. D. Diehl and R. McGrath, Surf. Sci. Rep. **23**, 43 (1996).
[3] K. Müller, G. Besold, and K. Heinz, in *Physics and Chemistry of Alkali Metal Adsorption*, edited by H. P. Bonzel, A. M. Bradshaw, and G. Ertl (Elsevier, Amsterdam, 1989), p. 65.
[4] H. Ishida and K. Terakura, Phys. Rev. B **36**, 4510 (1987).
[5] H. Ishida, Phys. Rev. B **38**, 8006 (1988).
[6] J. Neugebauer and M. Scheffler, Phys. Rev. Lett. **71**, 577 (1993).
[7] R. J. Behm, in *Physics and Chemistry of Alkali Metal Adsorption* (Ref. 3), p. 111.
[8] A. Cucchetti, Ph.D. thesis, Brown University, Rhode Island, 1996.
[9] K. Wandelt, *Physics and Chemistry of Alkali Metal Adsorption* (Ref. 3), p. 25.
[10] K. Horn, J. Somers, Th. Lindner, and A. M. Bradshaw, *Physics and Chemistry of Alkali Metal Adsorption* (Ref. 3), p. 55.
[11] S. Mizuno, H. Tochihara, and T. Kawamura, Phys. Rev. B **50**, 17 540 (1994).
[12] C. Astaldi, P. Rudolf, and S. Modesti, Solid State Commun. **75**, 847 (1990).
[13] J. Ellis and J. P. Toennies, Phys. Rev. Lett. **70**, 2118 (1993).
[14] G. Benedek, J. Ellis, A. Reichmuth, P. Ruggerone, H. Schief, and J. P. Toennies, Phys. Rev. Lett. **69**, 2951 (1992).
[15] N. S. Luo, P. Ruggerone, J. P. Toennies, G. Benedek, and V. Celli, J. Electron Spectrosc. Relat. Phenom. **64/5**, 755 (1993).
[16] G. Witte, Ph.D. thesis, University of Göttingen, 1995.
[17] B. Poelsema and G. Comsa, *Scattering of Thermal Energy Atoms from Disordered Surfaces* (Springer-Verlag, Heidelberg, 1989).
[18] While there is no direct evidence from other studies concerning the coverage dependence of the sticking coefficient for Na/Cu(001), the measurements of Argile and Rhead [C. Argile and G. E. Rhead, Surf. Sci. **279**, 244 (1992)] show a constant submonolayer sticking coefficient for K/Cu(001), indicating that this is also likely to be the case for Na/Cu(001).
[19] F. Hofmann and J. P. Toennies, Chem. Rev. **96**, 1307 (1996).
[20] F. Hofmann, J. R. Manson, and J. P. Toennies, J. Chem. Phys. **101**, 10 155 (1994).
[21] J. P. Toennies, *Surface Phonons*, edited by F. de Wette, Springer Series in Surface Sciences Vol. 14 (Springer-Verlag, Heidelberg, 1988), p. 248.
[22] G. Benedek, J. Ellis, N. S. Luo, A. Reichmuth, P. Ruggerone, and J. P. Toennies, Phys. Rev. B **48**, 4917 (1993).
[23] A. P. Graham, M. F. Bertino, F. Hofmann, and J. P. Toennies, J. Phys. Chem. **100**, 19 136 (1996).
[24] A. P. Graham, F. Hofmann, J. P. Toennies, L. Y. Chen, and S. C. Ying, Phys. Rev. Lett. **78**, 3900 (1997); A. P. Graham, F. Hofmann, J. P. Toennies, L. Y. Chen, and S. C. Ying, Phys. Rev. B **56**, 10 567 (1997).

[25] A. P. Graham, P. Senet, and J. P. Toennies (unpublished).
[26] L. Y. Chen and S. C. Ying, Phys. Rev. Lett. **71**, 4361 (1993).
[27] J. Ellis and J. P. Toennies, Surf. Sci. **317**, 99 (1994).
[28] T. Aruga, H. Tochihara, and Y. Murata, Phys. Rev. Lett. **52**, 1794 (1984).
[29] H. Wedler, M. A. Mendez, P. Bayer, U. Löffler, K. Heinz, V. Fritzsche, and J. B. Pendry, Surf. Sci. **293**, 47 (1993).
[30] B. F. Mason and B. R. Williams, Surf. Sci. **75**, L786 (1978).
[31] R. L. Gerlach and T. N. Rhodin, Surf. Sci. **17**, 32 (1969).
[32] N. D. Shrimpton, G. S. Welsh, and J. Song, Phys. Rev. B **45**, 1403 (1992).
[33] D. Fisher and R. D. Diehl, Phys. Rev. B **46**, 2512 (1992).
[34] A. G. Naumovets, Surf. Sci. **299/300**, 706 (1994); A. G. Naumovets, in *The Chemical Physics of Solid Surfaces*, edited by D. A. King and D. P. Woodruff (Elsevier, Amsterdam, 1994), Vol. 7, p. 163.
[35] D. Vanderbilt, Surf. Sci. **268**, L300 (1992).
[36] K.-O. Ng and D. Vanderbilt, Phys. Rev. B **52**, 2177 (1995).
[37] K. Kern, H. Niehus, A. Schatz, P. Zeppenfeld, J. Goerge, and G. Comsa, Phys. Rev. Lett. **67**, 855 (1991).
[38] P. Senet, J. P. Toennies, and G. Witte (unpublished).